

Stability of Multi-Microgrids: New Certificates, Distributed Control, and Braess's Paradox

Amin Gholami, *Student Member, IEEE* and Xu Andy Sun, *Senior Member, IEEE*

Abstract—This paper investigates the theory of resilience and stability in multi-microgrid (multi- μ G) networks. We derive new sufficient conditions to guarantee small-signal stability of multi- μ Gs in both lossless and lossy networks. The new stability certificate for lossy networks only requires local information, thus leads to a fully distributed control scheme. Moreover, we study the impact of network topology, interface parameters (virtual inertia and damping), and local measurements (voltage magnitude and reactive power) on the stability of the system. The proposed stability certificate suggests the existence of Braess's Paradox in the stability of multi- μ Gs, i.e. adding more connections between microgrids could worsen the multi- μ G system stability as a whole. We also extend the presented analysis to structure-preserving network models, and provide a stability certificate as a function of original network parameters, instead of the Kron reduced network parameters. We provide a detailed numerical study of the proposed certificate, the distributed control scheme, and a coordinated control approach with line switching. The simulation shows the effectiveness of the proposed stability conditions and control schemes in a four- μ G network, IEEE 33-bus system, and several large-scale synthetic grids.

I. INTRODUCTION

RESTRUCTURING of distribution systems into multi-microgrids (multi- μ Gs) is one of the main ways of improving the resilience of the electricity grid. The structural modularity of such networks makes them remarkably resilient against extreme events, but inherently prone to instabilities nonetheless. A minor contingency in these networks may lead to cascading outages and a total blackout in all microgrids. There is, therefore, an urgent need for understanding the notion of stability in multi- μ Gs. The present paper is motivated by this urgent need and is aimed at characterizing the conditions under which a multi- μ G is locally stable. We also attempt to understand how the topology and parameters of the network would affect the stability of a multi- μ G, and how we can monitor and guarantee its stability using a distributed control scheme.

A key feature that distinguishes future multi- μ G networks from the conventional distribution systems is that each microgrid will be connected to the rest of the system via a point of common coupling (PCC). Moreover, each microgrid either has a voltage source inverter (VSI)-based interface at PCC or is composed of a network of distributed energy resources (DERs), e.g. VSIs, diesel generators (DGs), etc [1], [2]. On the other hand, it can be mathematically proved (see Lemma 1) that the frequency dynamics of a droop-controlled VSI

is equivalent to the dynamics of a synchronous generator or DG, represented by swing equations [3], [4]. Therefore, from a modeling perspective, the dynamical model of multi- μ Gs is closely related to that of interconnected generators [5], and analysis of multi- μ Gs' behaviour is intertwined with an accurate understanding of swing equations.

Swing equations with zero transfer conductances (the so-called *lossless* model) have been studied in the 1980s (see e.g. [6]). Various methods in the broad category of the so-called direct methods have been developed to estimate the region of attraction of equilibrium points (EPs) and conduct transient stability analysis [7], [8]. Unfortunately, the existing direct methods are mostly cumbersome and limited to lossless systems. In a similar vein, the method in [9] algorithmically constructs Lyapunov functions for swing equations using semidefinite programming and sum of squares decomposition. Nevertheless, there are serious numerical difficulties with applying such methods to large power systems. More recently, some of these numerical problems are partially overcome by system decomposition [10], or by showing that there exists a convex set of Lyapunov functions certifying the transient stability of a given power system, and then finding the best suited Lyapunov function in the family to a specific contingency [11].

Swing equations with nonzero transfer conductances (the so-called *lossy* model) are more challenging to analyze. This is partly because there is no global energy function for such systems [12], and therefore, some basic techniques (e.g., the energy function method) for studying these equations cannot be directly applied. Nonetheless, several workarounds are developed over the years [9], [10], [13]–[18]. For instance, the method in [15] constructs Lyapunov functions for lossy swing equations using dissipative systems theory. However, the method still needs to be highly tuned to converge and has limitations on the bus angle differences. Athay *et al.* in [16] propose a method to estimate critical clearing times associated with first swing transient instability without explicitly solving any differential equations. The method was not supported by a sound theory at the time, but later in [17], a theory is also developed to support the method using the ideas of extended invariance principle.

In [19], the lossy swing equation model is extended by considering the dynamics of the excitation system, and the asymptotic stability of EPs is ensured by proving the existence of Lyapunov functions and designing a nonlinear feedback control for the generator excitation field. The approach in [19] is based on the assumption that the line transfer conductances are sufficiently small, and the angle differences at EPs are also small. Our approach in this paper does not require these two

The authors are with the H. Milton Stewart School of Industrial and Systems Engineering, Georgia Institute of Technology, Atlanta, GA 30332 USA (e-mail: a.gholami@gatech.edu; andy.sun@isye.gatech.edu).

assumptions and is aimed at finding a real-time certificate for the local stability (as opposed to global stability in [19]) of EPs.

In [20], the local stability of swing equations with nontrivial transfer conductances is examined by linearization, and conditions for stability of EPs are established. It is also shown that undamped swing equations can be stable only under very special circumstances. Contrary to [20], the stability certificate for lossy networks in the present paper can be evaluated using only local measurements, does not require a reference bus, and reveals new relationships between network topology and stability of EPs.

Swing equations can also be studied from a graph-theoretic perspective, where the main focus is on investigating the relationship between the underlying graph structure of the power system and the system stability [21]–[25]. Our work in this paper falls into this research category. We refer to [24] and [25] for a comprehensive survey on this topic. In particular, the existing results on the small-signal stability of lossless swing equations are reviewed and studied in [24]. It is shown that if bus angle differences at an EP are less than $\pi/2$, then the EP is locally asymptotically stable. The present paper provides a generalization of such results to lossy swing equations. Contrary to the lossless case, we will show that an EP in lossy networks could be unstable even if bus angle differences are less than $\pi/2$.

Swing equations also play an important role in studying droop-controlled inverters in microgrids. In the literature, various models with different complexities have been adopted for droop-controlled inverters, including first-order models [26], second-order models [1], [3], [5], third-order models [27], and higher-order models [28]–[30]. Each model is useful for studying a particular aspect of droop-controlled inverters such as their frequency stability, voltage stability, or electromagnetic transients. The application of swing equations is more common in second-order models and frequency stability [3], [5]. Swing equations with variable voltage magnitudes also appear in third-order models. For instance, in [27], each inverter is modeled by a third-order differential equation including swing equations with variable voltage magnitudes. Using this model, sufficient conditions are derived for boundedness of trajectories in lossy microgrids as well as asymptotic stability of EPs in lossless microgrids. In the present paper, we focus on frequency stability and adopt a second-order model with constant voltage magnitudes for each inverter. In comparison with [27], in the lossless case, our results match the results of [27], See Remark 5.11]. In the lossy case, our sufficient condition in this paper certifies the asymptotic stability of EPs instead of boundedness of trajectories as in [27]. Nonetheless, our model for inverters here is different, and a direct comparison seems unfair.

The framework in [28] (and the follow-up articles [29], [30]) utilizes a more detailed dynamical model for inverter-based microgrids, modeling the droop-based frequency and voltage controls as well as the electromagnetic transients of power lines. After performing a model order reduction and constructing a Lyapunov function for the reduced model, a set of decentralized sufficient conditions are developed for

guaranteeing the small-signal stability of the EPs. In the present paper, we pursue the same goal as in [28]–[30], i.e., finding decentralized sufficient conditions for small-signal stability. However, our focus is more on frequency stability, and deriving more explicit stability conditions that reveal the role of network topology and parameters in small-signal stability.

The small-signal stability of multi- μ Gs is studied in [1], where various control frameworks are proposed for the microgrids' interface. Moreover, a plug-and-play rule is proposed in [5], guaranteeing the stability of multi- μ Gs without requiring the global knowledge of network topology or operating conditions.

The multi- μ G model in the present paper is similar to the one in [5], except we do not incorporate a local integral control. Corollary 1 in the present paper matches the plug-and-play rule in [5]. Moreover, the main result in Theorem 1 generalizes the main result of [5] because our stability certificate considers the real-time operating condition of the system and is less conservative. Our result is also a generalization of the result in [3] as we do not require uniform damping of inverters.

Another set of literature that are conceptually related to our work are the recent studies on power grid synchronization [31], frequency control [32], [33], voltage stability [34], and also the study of Kuramoto oscillators which has been linked to the stability analysis of lossy power systems with strongly overdamped generators [35].

This paper is a significant extension to our work presented in [36] on a certificate for local stability of lossy swing equations. Compared to [36], here we further extend the certificate as a function of network physical measurements, analyze and provide a proof for the lossless case, generalize the presented analysis to structure-preserving network models, discuss the physical interpretation and Braess's Paradox behind it, establish a distributed control scheme based on it, and finally show its application in multi- μ G networks. The main contributions of the present paper can be summarized below.

- **Stability Certificates:** We derive explicit sufficient conditions that certify small-signal stability of multi- μ Gs for both lossless and lossy networks. The new certificates provide significant insights about the interplay between system stability and reactive power absorption, voltage magnitude at PCC, network topology, and interface parameters of each microgrid. We also introduce a new weighted directed graph to study the spectral properties of the multi- μ G Laplacian.
- **Distributed Control:** In addition to providing new insights into the theory of stability, the derived stability certificates use only local information and are suitable for real-time monitoring and fast stability assessment. Based on the developed theory, we introduce a fully distributed control scheme to adjust the dynamic parameters of each microgrid interface for maintaining the stability of the system.
- **Analog of Braess's Paradox:** The stability conditions developed in this paper surprisingly reveal an analog of Braess's Paradox in power system stability, showing

that adding power lines to the system may decrease the stability margin [37]. The current paper rigorously establishes the impact of switching-off lines, increasing damping, and decreasing virtual inertia on improving system stability.

- **Generalization to Structure-Preserving Models:** We extend the presented analysis to structure-preserving power network models. Specifically, we prove a monotonic relationship between entries of a nodal admittance matrix and its Kron reduced counterpart. This monotonic relationship enables us to derive a stability condition as a function of original network parameters, instead of the Kron reduced network parameters. This is beneficial to real-time distributed control as the network parameters constantly change and Kron reduction may not be available to individual controllers.

We believe the findings in this paper are also applicable to other problems whose models display similar structural properties, such as small-signal stability assessment in the transmission level and synchronization of coupled second-order nonlinear oscillators. The rest of our paper is organized as follows. Section II provides a brief background on multi- μ Gs. In Section III, the multi- μ G model is linearized and several properties of the Jacobian matrix are proved. Section IV is devoted to the main results on sufficient conditions for the stability of multi- μ Gs. Section V further illustrates the developed analytical results through numerical examples, and finally, the paper concludes with Section VI.

II. BACKGROUND

A. Notations

We use \mathbb{C}_- to denote the set of complex numbers with negative real part, and \mathbb{C}_0 to denote the set of complex numbers with zero real part. $j = \sqrt{-1}$ is the imaginary unit. The spectrum of a matrix $A \in \mathbb{R}^{n \times n}$ is denoted by $\sigma(A)$. For $A \in \mathbb{C}^{n \times n}$ and $\alpha, \beta \subseteq \{1, \dots, n\}$, the submatrix of entries in the rows indexed by α and columns indexed by β is denoted by $A[\alpha, \beta]$. Similarly, for a vector $x \in \mathbb{C}^n$, $x[\alpha]$ denotes the subvector consisting of entries indexed by α .

B. Multi-Microgrid Model

Consider a distribution network represented as an undirected graph $\mathcal{G} = (\mathcal{N}, \mathcal{E})$, where \mathcal{N} is the set of nodes and \mathcal{E} is the set of edges. Each node in \mathcal{N} represents a microgrid and each edge in \mathcal{E} represents an electrical branch connecting the two microgrids across the branch. We will refer to \mathcal{G} as the linking grid [2]. The linking grid \mathcal{G} is *connected* if for any two nodes $i, k \in \mathcal{N}, i \neq k$ there exists a path between i and k consisting of power lines with nonzero admittance.

To begin the study, let us assume that each microgrid is modeled by a grid-forming VSI connected to a node of the linking grid. Given the time window of small-signal stability assessment, characterization of each microgrid by a VSI can be understood in two ways:

- 1) The first possibility is that a microgrid contains an ensemble of devices (e.g., grid-forming inverters, diesel

generators, and loads) whose aggregate behavior can be modeled by a VSI. The derivation of the aggregated VSI model is out of the scope of this paper. We refer to [38], [39] for details. Moreover, we restrict the type of microgrid DERs to grid-forming VSIs, DGs, and more generally to those whose dynamics can be captured by swing equations.

- 2) The second possibility is that a microgrid is connected to the linking grid through a grid-forming VSI at PCC [1], [2], [5]. VSI-based interfaces decouple the intra-microgrid dynamics from the grid side, and consequently, the interactions among different microgrids will be primarily determined by the VSI control law [1], [2].

When the model order reduction in way 1 introduces major errors, or VSI interfaces in 2 do not exist, it is inevitable that the internal structure, DERs, and loads of the microgrid be explicitly modeled. Later in Section IV-C, we will introduce a way to consider a structure-preserving model for each microgrid and extend our stability analysis to such cases. Let us for now focus on the case where each microgrid is represented as a node in the linking grid $\mathcal{G} = (\mathcal{N}, \mathcal{E})$ and modeled by a VSI.

Accordingly, the dynamics of a multi- μ G network is characterized by the following system of nonlinear autonomous ordinary differential equations (ODEs):

$$\dot{\delta}_i(t) = \omega_i(t) \quad \forall i \in \mathcal{N}, \quad (1a)$$

$$m_i \dot{\omega}_i(t) + d_i \omega_i(t) = P_{s_i} - P_{e_i}(\delta(t)) \quad \forall i \in \mathcal{N}, \quad (1b)$$

where for each microgrid $i \in \mathcal{N}$, P_{s_i} is the active power setpoint in per unit, P_{e_i} is the outgoing active power flow in per unit, m_i is the virtual inertia in seconds induced by the delay in droop control, d_i is the unitless damping coefficient, t is the time in seconds, $\delta_i(t)$ is the terminal voltage angle in radian, and finally $\omega_i(t)$ is the deviation of the angular frequency from the nominal angular frequency in radian per seconds. For the sake of simplicity, henceforth we do not explicitly write the dependence of the state variables δ and ω on time t .

The PCC of two microgrids i and k are connected via a power line with the admittance $y_{ik} = g_{ik} + jb_{ik}$, where $g_{ik} \geq 0$ and $b_{ik} \leq 0$. In transmission-level small-signal stability studies, the conductance g_{ik} of transmission lines is commonly assumed to be zero (aka lossless model). While this is a reasonable assumption in the transmission level, it may not hold in the distribution level and multi- μ G networks. Therefore, our analysis will be based on the general lossy case, and we discuss the lossless model as a special case. Let y_{ii} denote the admittance-to-ground at PCC i and define the symmetric admittance matrix given by the diagonal elements $Y_{ii} \angle \theta_{ii} = \sum_{k=1}^n y_{ik}$ and off-diagonal elements $Y_{ik} \angle \theta_{ik} = -y_{ik}$. Based on this definition, the function P_{e_i} in (1b) can be further spelled out:

$$P_{e_i}(\delta) = \sum_{k=1}^n V_i V_k Y_{ik} \cos(\theta_{ik} - \delta_i + \delta_k), \quad (2)$$

where V_i is the PCC terminal voltage magnitude of microgrid i .

Definition 1 (flow function). *The smooth function $P_e : \mathbb{R}^n \rightarrow \mathbb{R}^n$ given by $\delta \mapsto P_e(\delta)$ in (2) is called the flow function.*

The smoothness of the flow function (it is \mathcal{C}^∞ indeed) is a sufficient condition for the existence and uniqueness of the solution to the ODE (1). The flow function is translationally invariant with respect to the operator $\delta \mapsto \delta + \alpha \mathbf{1}$, where $\alpha \in \mathbb{R}$ and $\mathbf{1} \in \mathbb{R}^n$ is the vector of all ones. In other words, $P_e(\delta + \alpha \mathbf{1}) = P_e(\delta)$. A common way to deal with this situation is to define a reference bus and refer all other bus angles to it. This is equivalent to projecting the original state space onto a lower dimensional space.

Observe that EPs of the multi- μ G dynamical system (1) are of the form $(\delta^*, \omega^*) \in \mathbb{R}^{2n}$ where δ^* is a solution to the active power flow problem $P_{e_i}(\delta^*) = P_{s_i}, \forall i \in \mathcal{N}$ and $\omega^* = 0$. We seek an answer to the following question: under what conditions is an EP (δ^*, ω^*) locally asymptotically stable? A perfect answer to this question should give us a purely algebraic condition, shedding light on the relation between the stability of the EP and the parameters of system (1) (i.e., the interface parameters m_i and d_i , the setpoints P_{s_i} , and the underlying graph of the multi- μ G network). The rest of this paper is devoted to finding such an answer.

As mentioned before, model (1) is identical to the well-known swing equation model describing the dynamics of interconnected synchronous generators [40], and this is because VSI control schemes are widely devised to emulate the behavior of synchronous machines [1], [2], [4]. Indeed, the equivalence of the dynamics of synchronous generators and droop-controlled VSIs can be rigorously formalized. Specifically, a droop-controlled VSI at node $i \in \mathcal{N}$ can be modeled as [3]:

$$\dot{\delta}_i(t) = -k_i (P_{m_i}(t) - P_{d_i}), \quad (3a)$$

$$\tau_i \dot{P}_{m_i}(t) = -P_{m_i}(t) + P_{e_i}, \quad (3b)$$

where $k_i \geq 0$ is the droop gain, $P_{m_i} \in \mathbb{R}$ is the measured active power, $P_{d_i} \in \mathbb{R}$ is the desired active power setpoint, and $\tau_i \geq 0$ is the time constant of the low-pass filter of the power measurement. Now, the next lemma shows the droop-controlled VSI model (3) can be reparametrized as the swing equation model (1).

Lemma 1 (VSI model reparametrization). *The dynamics of the droop-controlled VSI model (3) is equivalent to the dynamics of the swing equation model (1).*

Proof. Consider the VSI model (3) and define the new variable $\omega_i(t)$ as

$$\omega_i(t) := \dot{\delta}_i(t) = -k_i (P_{m_i}(t) - P_{d_i}). \quad (4)$$

Thus, using the new variable $\omega_i(t)$, equation (3a) can be written as (1a). By substituting $P_{m_i}(t) = -\omega_i(t)/k_i + P_{d_i}$ into (3b), we get

$$-\tau_i \dot{\omega}_i(t)/k_i = \omega_i(t)/k_i - P_{d_i} + P_{e_i}.$$

Now, for each node $i \in \mathcal{N}$, define the virtual inertia coefficient $m_i := \tau_i/k_i$, virtual damping $d_i := 1/k_i$, and active power setpoint $P_{s_i} := P_{d_i}$. Therefore, (3b) is equivalent to (1b). \square

Similar derivations can be found for example in [3], [41]. Accordingly, the application of model (1) is not restricted to the characterization of interconnected microgrids. The model (and consequently, the results developed in this paper) can be applied to a system of interconnected synchronous machines, coupled oscillators, etc.

III. LINEARIZATION AND SPECTRUM OF JACOBIAN

A. Linearization

Let us take the state variable vector $(\delta, \omega) \in \mathbb{R}^{2n}$ into account and note that the first step in studying the stability of multi- μ G EPs is to analyze the Jacobian of the vector field in (1):

$$J := \begin{bmatrix} 0 & I \\ -M^{-1}L & -M^{-1}D \end{bmatrix} \in \mathbb{R}^{2n \times 2n} \quad (5)$$

where $I \in \mathbb{R}^{n \times n}$ is the identity matrix, $M = \text{diag}(m_1, \dots, m_n)$, and $D = \text{diag}(d_1, \dots, d_n)$. Throughout the paper, we assume M and D are nonsingular. Moreover, $L \in \mathbb{R}^{n \times n}$ is the Jacobian of the flow function with the entries:

$$L_{ii} = \sum_{k=1, k \neq i}^n V_i V_k Y_{ik} \sin(\theta_{ik} - \delta_i + \delta_k), \forall i \in \mathcal{N} \quad (6a)$$

$$L_{ik} = -V_i V_k Y_{ik} \sin(\theta_{ik} - \delta_i + \delta_k), \forall i \neq k \in \mathcal{N}. \quad (6b)$$

The matrix L plays a prominent role in the spectrum of the Jacobian matrix J (and as a consequence, in the stability properties of the EPs of multi- μ Gs). We illustrate this role in the following subsection.

B. Spectral Relationship Between Matrices J and L

The next lemma shows that the eigenvalues of J and L are linked through a singularity constraint. Recall that for $n \times n$ real matrices Q_0, Q_1 , and Q_2 , a *quadratic matrix pencil* is a matrix-valued function $P : \mathbb{C} \rightarrow \mathbb{R}^{n \times n}$ given by $\lambda \mapsto P(\lambda)$ such that $P(\lambda) = \lambda^2 Q_2 + \lambda Q_1 + Q_0$.

Lemma 2. *λ is an eigenvalue of J if and only if the quadratic matrix pencil $P(\lambda) := \lambda^2 M + \lambda D + L$ is singular.*

The proof of Lemma 2 is given in [36]. Next, Proposition 1 illustrates the relationship between the kernels and the multiplicity of the zero eigenvalue of the two matrices J and L .

Proposition 1. *Consider the Jacobian matrix J in (5). The following statements hold:*

- (i) *The kernel of L is the orthogonal projection of the kernel of J onto the linear subspace $\mathbb{R}^n \times \{0\}$. That is, $\ker(L) = \text{proj}(\ker(J))$.*
- (ii) *The geometric multiplicity of the zero eigenvalue in $\sigma(J)$ and $\sigma(L)$ are equal.*
- (iii) *J is nonsingular if and only if L is nonsingular.*

Proof. See Appendix A. \square

As the role of L in the spectrum of J became more clear, we scrutinize the spectrum of L in the next subsection. Our

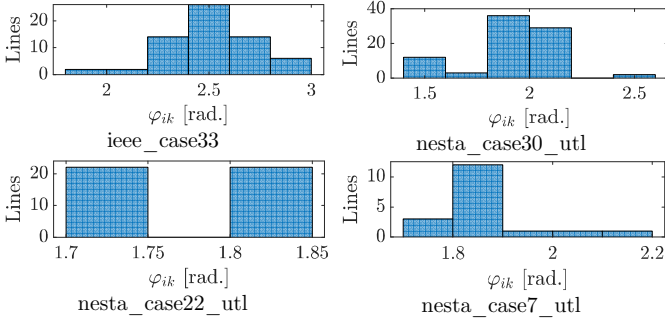


Fig. 1: Histogram of the distribution of φ_{ik} for all lines (i, k) in different IEEE and NESTA standard test cases.

final goal is to use the spectral properties of L together with the relationships established in Lemma 2 and Proposition 1 to derive a stability certificate for multi- μ Gs.

C. A Directed Graph Induced by L

The linking grid of a multi- μ G is represented by the undirected graph \mathcal{G} defined in Section II-B. However, to fully represent the Jacobian L of the flow function (2), we need to introduce a new *weighted directed graph* (digraph). Let $\vec{\mathcal{G}} = (\mathcal{N}, \mathcal{A}, \mathcal{W})$, where each node $i \in \mathcal{N}$ corresponds to a microgrid and each directed arc $(i, k) \in \mathcal{A}$ corresponds to the entry $(i, k), i \neq k$ of the admittance matrix. We further define a weight for each arc $(i, k) \in \mathcal{A}$:

$$w_{ik} = V_i V_k Y_{ik} \sin(\varphi_{ik}), \quad (7)$$

where $\varphi_{ik} := \theta_{ik} - \delta_i + \delta_k$. With the above definitions, we can see that the Jacobian matrix L of the flow function, which appeared in (6), is indeed the *Laplacian* of the weighted digraph $\vec{\mathcal{G}}$. In general, the arc weights w_{ik} can take any values in \mathbb{R} , and the matrix L is not necessarily symmetric. In practice, however, w_{ik} varies in a small nonnegative range. Figure 1 illustrates the histogram of the angle φ_{ik} for all lines (i, k) in different IEEE and NESTA standard distribution test cases, where the converged load flow data are obtained from MATPOWER [42]. Accordingly, $\varphi_{ik} \in (0, \pi)$ in all of these cases. Thus, it is reasonable to assume that the EPs (δ^*, ω^*) of the multi- μ G dynamical system (1) are located in the set Ω defined as

$$\Omega = \left\{ (\delta, \omega) \in \mathbb{R}^{2n} : 0 < \theta_{ik} - \delta_i + \delta_k < \pi, \forall (i, k) \in \mathcal{A}, \omega = 0 \right\}.$$

Under this assumption, the arc weights $w_{ik} > 0$ for all arcs (i, k) . So, there are two arcs (i, k) and (k, i) between microgrids i and k if and only if the two microgrids are physically connected. We always assume the physical network connecting all the microgrids is a connected (undirected) graph. The weighted digraph $\vec{\mathcal{G}}$ will be used to study the spectral properties of L .

D. Spectral Properties of L

When φ_{ij} 's satisfy the above angle assumption, the following proposition from [36] shows that L is a singular M-matrix. Moreover, the zero eigenvalue of L is simple, i.e.

the algebraic and geometric multiplicities are one, which is important for preventing bifurcation from happening in the multi- μ grid network.

Proposition 2. *Let $(\delta^*, \omega^*) \in \Omega$ be an EP of the multi- μ G system (1). Assume the linking grid \mathcal{G} is connected. The Jacobian matrix L defined by (6) at this EP has the following properties:*

- (i) *L has a zero eigenvalue with an eigenvector $\mathbf{1}$, and the real part of each nonzero eigenvalue of L is positive, i.e. L is a singular M-matrix.*
- (ii) *The zero eigenvalue of L is simple.*

Properties (i) and (ii) of L shown in the above proposition will be used in the next section to prove the stability of J in the main result of the paper.

IV. STABILITY OF MULTI-MICROGRID NETWORKS

Now we are ready to answer the fundamental question posed in Section II-B: under what conditions is an EP (δ^*, ω^*) locally asymptotically stable?

A. The Main Stability Theorem

Theorem 1. *Let $(\delta^*, \omega^*) \in \Omega$ be an EP of the multi- μ G system (1). Let $B \in \mathbb{R}^{n \times n}$ denote the imaginary part of the admittance matrix. Suppose all microgrid interfaces have positive damping coefficient and inertia, and the linking grid \mathcal{G} is connected. Then, the following statements hold:*

- (a) *The Jacobian J at this EP has a zero eigenvalue with geometric multiplicity of one.*
- (b) *All the nonzero real eigenvalues of J are negative.*
- (c) *Let Q_i be the net outgoing reactive power flow from microgrid PCC i . If*

$$-Q_i - V_i^2 B_{ii} \leq \frac{d_i^2}{2m_i}, \quad \forall i \in \mathcal{N} \quad (8)$$

- then all the nonzero eigenvalues of J , both real and complex, are located in the left half plane, i.e., $\sigma(J) \subset \mathbb{C}_- \cup \{0\}$, and the EP is locally asymptotically stable.*
- (d) *If the transfer conductance of the lines is zero, then all the nonzero eigenvalues of J are located in the left half plane, and the EP is locally asymptotically stable.*

Proof. See Appendix B. □

Remark 1. *Properties (a) and (b) hold independently of the sufficient conditions in (c) and (d). Property (d) says if the network is lossless, then regardless of (c), any EP is stable. If instead the network is lossy, then not every EP is stable and condition (8) provides a new certificate to guarantee the small-signal stability of an EP.*

Remark 2. *Notice that a salient feature of condition (8) is that it only requires local information at each microgrid interface, hence, leads to a fully distributed control scheme to stabilize the multi- μ G system. Detailed numerical simulation will be shown in Section V.*

B. Intuition and Paradox Behind Condition (8)

Condition (8) in Theorem 1 provides a practical and efficient way to certify the stability of the EPs in general lossy multi- μ G networks. It also introduces a distributed control rule for tuning the interface parameters of each microgrid without compromising the network stability. In this section, we will explore the intuition behind this theory as well as two interesting paradoxes that come with it.

- **Note 1:** The variable Q_i in (8) is the net reactive power that microgrid i injects into the rest of the multi- μ G network, that is, if microgrid i is supplying reactive power, then $Q_i > 0$. Otherwise, if it is consuming reactive power, then $Q_i < 0$. Intuitively, when microgrid i is a supplier of reactive power, the first term on the left-hand side of (8) is negative, and this situation will help condition (8) hold.
- **Note 2:** Recall that $Y_{ii} \angle \theta_{ii} = G_{ii} + jB_{ii} = \sum_{k=1}^n y_{ik}$, where $y_{ik} = g_{ik} + jb_{ik}$ is the admittance of line (i, k) , with $g_{ik} \geq 0$ and $b_{ik} \leq 0$. Therefore, $B_{ii} \leq 0$, and the second term on the left-hand side of (8) is always positive. Here, it is assumed that y_{ii} , i.e., the admittance-to-ground at PCC i is negligible. Otherwise, we may have $B_{ii} > 0$, and the second term on the left-hand side of (8) could be negative.
- **Note 3:** The first two notes clarify that the left-hand side of (8) can be negative if microgrid i is supplying reactive power; otherwise it is positive. Consequently, condition (8) is not trivial.
- **Note 4:** Condition (8) enforces an upper bound which is proportional to the square of damping and inverse of inertia. This is consistent with the intuition that if we increase the damping, the stability margin of the system will increase. However, it is not intuitive (could be a paradox) that decreasing the virtual inertia of a microgrid interface will increase the stability margin.
- **Note 5:** By adding more transmission lines to the system, $|B_{ii}|$ will increase, and this in turn could increase the left-hand side of (8) and lead to the violation of this condition. This can be called the Braess's Paradox in power system stability.

The following corollary will further illustrate the aforementioned Braess's Paradox.

Corollary 1. Under the assumptions of Theorem 1, if

$$\sum_{k=1, k \neq i}^n V_i V_k Y_{ik} \leq \frac{d_i^2}{2m_i}, \quad \forall i \in \mathcal{N} \quad (9)$$

then the nonzero eigenvalues of J are located in the left half plane and the EP is locally asymptotically stable.

This corollary directly follows from the proof of Theorem 1 provided in Appendix B. Counterintuitively, according to (9), adding more power lines can lead to violating the sufficient condition for stability. This Braess's Paradox in power systems has been also acknowledged in [43] and [5] in different contexts and using different approaches. Note that removing lines from a network could make the system more vulnerable to contingencies and eliminate the reliability benefits of having

more transmission line capacity. This trade-off should be taken into account during the design and operation of power grids.

C. Stability Condition in Structure-Preserving Networks

1) *Motivation:* The stability certificate (8) in Section IV-A is derived for the linking grid $\mathcal{G} = (\mathcal{N}, \mathcal{E})$, where each microgrid is reduced to one node modeled as a grid-forming inverter using the swing equation. In this section, we consider the more general situation, where the internal active and passive elements of a microgrid are explicitly modeled. In particular, let $\mathcal{G}^d = (\mathcal{N}^d, \mathcal{E}^d)$ be the distribution network composed of all microgrids $\mathcal{G}_i = (\mathcal{N}_i, \mathcal{E}_i)$ for $i \in \mathcal{N}$ as subnetworks. The buses \mathcal{N}_i of microgrid i may include both active nodes (i.e., those connected to DGs and/or VSIs) and passive nodes (i.e., those connected to a constant admittance load).

In order to study the stability property of \mathcal{G}^d , we first use Kron reduction to eliminate all passive nodes from each microgrid and study the resulting reduced network \mathcal{G}^r . The stability condition (8) can be applied to \mathcal{G}^r . However, such a certificate is expressed in the system states and parameters of \mathcal{G}^r , not of the original network \mathcal{G}^d . This is not desirable, as it obscures the relations between the topology of the original network and the stability properties of the EPs. Moreover, the parameters of the Kron-reduced network \mathcal{G}^r may not be available to the individual microgrid controllers in real time. We want to find a stability certificate for the Kron-reduced network \mathcal{G}^r , expressed in the system states and network topology of the original network \mathcal{G}^d .

To tackle this challenge, we first identify in Section IV-C2 a sufficient condition on the admittances of the original network \mathcal{G}^d , under which certain monotonic relationship between the admittances of \mathcal{G}^d and \mathcal{G}^r can be obtained. Then in Section IV-C3, we use this monotonicity property to derive a stability certificate expressed directly in states and parameters of \mathcal{G}^d .

2) The Kron-Reduced and Original Networks:

Definition 2. Let Y be the nodal admittance matrix of a microgrid $\mathcal{G}_i = (\mathcal{N}_i, \mathcal{E}_i)$, where the set of active and passive nodes are denoted by $\alpha, \beta \subseteq \mathcal{N}_i$, respectively. The Kron reduction of \mathcal{G}_i that eliminates all nodes in β has an admittance matrix given by $Y^r := Y[\alpha, \alpha] - Y[\alpha, \beta]Y[\beta, \beta]^{-1}Y[\beta, \alpha]$. This Kron-reduced network is denoted by \mathcal{G}_i^r .

Assumption 1 below is widely satisfied in distribution grids.

Assumption 1. The nodal admittance matrix $Y = G + jB$ of a distribution grid satisfies $G_{ik} \leq 0, B_{ik} \geq 0$, for all $i \neq k$, and $G_{ii} \geq 0, B_{ii} \leq 0$ for self-admittances.

Assumption 2 below is the sufficient condition used in Lemma 3 to derive a monotonicity relation between the admittances of the original and Kron-reduced networks.

Assumption 2. Let $Y = G + jB$ be the nodal admittance matrix of a distribution grid. There exist two fixed real numbers ν_{\min} and ν_{\max} that satisfy

$$0 \leq \nu_{\min} \leq \nu_{\max} \leq \sqrt{1 + 2\nu_{\min}^2} \quad (10)$$

such that, for every line (i, k) , the conductance G_{ik} and susceptance B_{ik} are bounded as

$$\nu_{\min}|G_{ik}| \leq |B_{ik}| \leq \nu_{\max}|G_{ik}|. \quad (11)$$

Remark 3. By (11), if $G_{ik} = 0$, then $B_{ik} = 0$; otherwise, $\nu_{\min} \leq |B_{ik}|/|G_{ik}| \leq \nu_{\max}$, where the upper and lower bounds satisfy (10). As an example, if $\nu_{\min} = 5$, then we can set $\nu_{\max} = \sqrt{1 + 2 \cdot 5^2} = 7.14$. Then, according to (11), all lines have $|B_{ik}|/|G_{ik}|$ ratio between 5 and 7.14, which is typical in distribution grids, especially in microgrids.

Lemma 3. Suppose the nodal admittance matrix $Y = G + jB$ of a distribution grid satisfies Assumptions 1 and 2 and the Kron-reduced matrix $Y^r = G^r + jB^r$ from eliminating a passive node $k_0 \in \mathcal{N}_i$ satisfies Assumption 2. Then, Y^r also satisfies Assumption 1. Furthermore, the monotonicity condition, $B_{kk}^r \geq B_{kk}$, holds for all nodes $k \neq k_0$.

See Appendix C for the proof of this lemma.

3) *Stability Condition as a Function of Original Network:* Recall that the Kron-reduced network \mathcal{G}^r is obtained by Kron-reducing all passive nodes in all the microgrids. So \mathcal{G}^r only contains active nodes and its dynamical system is defined by model (1), where each active node has a swing equation. The next theorem is the key result of this section that states a stability certificate for \mathcal{G}^r but expressed in the states, network topology, and parameters of the original multi- μG , where microgrids are allowed to have an arbitrary internal structure with DGs, grid-forming inverters, and passive loads.

Theorem 2. Suppose Assumption 1 holds for all the microgrids $\mathcal{G}_i = (\mathcal{N}_i, \mathcal{E}_i)$ for $i \in \mathcal{N}$ in the distribution grid \mathcal{G}^d and Assumption 2 holds for the reduced admittance matrix of \mathcal{G}^d resulting from removing any passive node k_0 in \mathcal{G}_i for any $i \in \mathcal{N}$. Then an EP of the Kron-reduced grid \mathcal{G}^r is locally asymptotically stable, if the following condition holds

$$-Q_k - V_k^2 B_{kk} \leq \frac{d_k^2}{2m_k}, \quad \forall k \in \alpha_i, i \in \mathcal{N}, \quad (12)$$

where $\alpha_i \subseteq \mathcal{N}_i$ is the set of active nodes in microgrid \mathcal{G}_i and all quantities $Q_k, V_k, B_{kk}, d_k, m_k$ correspond to the original network \mathcal{G}^d .

The proof of this theorem is given in Appendix D.

V. COMPUTATIONAL EXPERIMENTS

In this section, we test various aspects of Theorems 1 and 2, and show how they can be used not only as a fast stability certificate, but also as a quantitative measure of the degree of stability. Furthermore, we demonstrate that condition (8) offers a distributed control rule to retain and ensure the stability of interconnected microgrids in an emergency situation. Let us define

$$\mathcal{S}_i := -Q_i - V_i^2 B_{ii} - \frac{d_i^2}{2m_i},$$

and recall that according to condition (8) in Theorem 1, if $\mathcal{S}_i \leq 0, \forall i \in \mathcal{N}$, then the EP of the multi- μG system is guaranteed to be asymptotically stable.

A. Control Schemes and Braess's Paradox

Consider the four-microgrid system shown in Fig. 2a and its load-flow and dynamical data tabulated in Case (a1) of Table I. The system is normally operating in this case, but $\mathcal{S}_i > 0, \forall i \in \mathcal{N}$ and Theorem 1 does not certify the stability of the system. Such a positive \mathcal{S}_i for all microgrids indicates that the multi- μG system, albeit operating normally, is close to its stability margins. We will show how a credible contingency could push such an uncertified system into instability.

Internal Outage Leads to Instability: Subsequent to a generation outage inside microgrid $\mu\mathcal{G}_4$, the active power P_{s_4} changes from -4.06 to -7.06 , i.e., this microgrid starts to get 3 p.u. more active power from the linking grid to compensate for its internal outage. In response, microgrid $\mu\mathcal{G}_3$ aids $\mu\mathcal{G}_4$ by using its internal generation capacity and changing its active power P_{s_3} from -2.25 to 0.25 . See Case (a2) in Table I. Such a smart, resilient, and self-healing multi- μG system seems very appealing and is indeed one of the main purposes of building these interconnected systems. However, as it was hinted by positive values of \mathcal{S}_i (i.e., violation of condition (8)), this new EP of the multi- μG system is unstable. The instability of this EP can be verified through eigenvalue analysis and time domain simulation, as depicted in Fig. 3. Now, Theorem 1 offers two remedial approaches to ensure system stability.

A Distributed Control Scheme: The first approach is based on a distributed control rule instructing how to change the interface controller parameters d_i or m_i in order to improve the multi- μG stability (recall the characterization of m_i and d_i for microgrids described in Section II-B). Based on local measurements of reactive power Q_i and voltage V_i , each microgrid can increase its damping d_i and/or decrease its virtual inertia to ensure that condition (8) is satisfied. The key features of the distributed control scheme include 1) by increasing d_i^2/m_i the system can always be stabilized according to condition (8); 2) the operating point of the system is not changed; 3) no information exchange from the neighboring microgrids is required. Implementing this approach, we reach to Case (a3) in Table I. The stability of the same EP as in Case (a2) is certified.

A Coordinated Control Scheme: The second approach offers coordination of a more general set of corrective actions including change of interface controller parameters d_i or m_i , change of reactive power Q_i or voltage magnitude V_i , and change of network topology. Condition (8) instructs which actions will improve the stability of the EP. The EP of the system may be moved in the coordinated control scheme to achieve corrective actions with smaller magnitude. To illustrate, we choose a combination of all available options to find a stable EP. Let us reconfigure the network by switching two lines off (see Fig. 2(b)) and also modify the dynamic parameters to reach Case (b) in Table I. The new EP satisfies condition (8) and therefore is stable. Note that by removing distribution lines from case (a), the value of $|B_{ii}|, \forall i \in \{1, 2, 4\}$ will decrease. Moreover, increasing damping and decreasing inertia will increase the right-hand side of (8). Consistent with Braess's Paradox, switching off two lines indeed improves system stability.

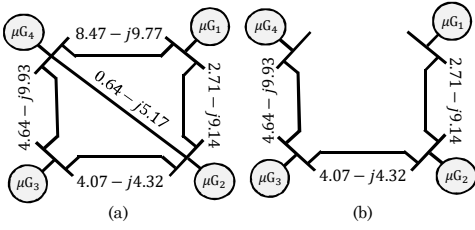


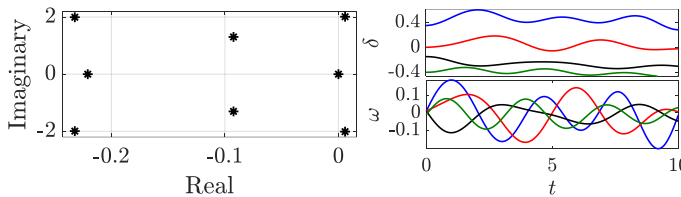
Fig. 2: Schematic diagram of four coupled microgrids.

TABLE I: Dynamic parameters and converged load flow data of the four-microgrid system.

| | i | m_i | d_i | P_{s_i} [p.u.] | V_i [p.u.] | δ_i^* [rad] | \mathcal{S}_i |
|-----------|-----|-------|-------|------------------|--------------|--------------------|-----------------|
| Case (a1) | 1 | 5.76 | 1.03 | 13.13 | 0.95 | 0.75 | 21.18 |
| | 2 | 9.20 | 1.61 | 0.39 | 0.95 | 0.28 | 16.85 |
| | 3 | 9.32 | 1.86 | -2.25 | 1.05 | -0.18 | 12.12 |
| | 4 | 4.92 | 1.50 | -4.06 | 1.05 | -0.07 | 16.12 |
| Case (a2) | 1 | 5.76 | 1.03 | 13.13 | 0.96 | 0.47 | 21.17 |
| | 2 | 9.20 | 1.61 | 0.39 | 0.95 | 0.07 | 16.50 |
| | 3 | 9.32 | 1.86 | 0.25 | 0.99 | -0.25 | 13.08 |
| | 4 | 4.92 | 1.50 | -7.06 | 1.02 | -0.37 | 13.53 |
| Case (a3) | 1 | 0.50 | 4.62 | 13.13 | 0.96 | 0.47 | -0.074 |
| | 2 | 0.56 | 4.32 | 0.39 | 0.95 | 0.07 | -0.035 |
| | 3 | 0.66 | 4.19 | 0.25 | 0.99 | -0.25 | -0.037 |
| | 4 | 0.56 | 3.92 | -7.06 | 1.02 | -0.37 | -0.001 |
| Case (b) | 1 | 0.80 | 4.03 | 5.72 | 1.05 | 0.8 | -0.0036 |
| | 2 | 0.56 | 3.90 | 0.40 | 1.05 | 0.24 | -0.0668 |
| | 3 | 0.70 | 3.78 | 0.25 | 1.05 | -0.62 | -0.0057 |
| | 4 | 0.68 | 3.49 | -2.11 | 0.95 | -0.8 | -0.0205 |

B. Stability Measure and Location of Eigenvalues

As mentioned above, condition (8) can be used not only as a fast stability certificate, but also as a quantitative measure of the degree of stability. To further illustrate this, consider the IEEE 33-bus network during islanded operation, consisting of 4 DGs and 2 storage units interfaced via VSIs [44]. The load, line, and DG data can be found in [42], [44], [45], and Table III. Here, we first compute the Kron-reduced system to obtain a network of interconnected DGs. Note that Theorem 2 is applicable to this reduced network because by Lemma 1 the dynamical model of interconnected droop-controlled VSIs can be reparametrized as the swing equation model (1). Observe that according to Fig. 1, the assumption $\varphi_{ik} \in (0, \pi)$ holds in this system. We assume the network is operating at 80% of the nominal load, and the interface parameters k_i , τ_i , m_i , d_i , and setpoints are designed following Theorem 2 (see Table



(a) Spectrum of matrix J . (b) Orbits of the system.

Fig. 3: Verifying the instability of the EP in Case (a2) of the four-microgrid system. (a) There exist two eigenvalues with positive real part. (b) Starting from a neighborhood of the EP, the orbits of the system diverge to infinity.

TABLE II: Parameters to generate synthetic networks. $U([\ell_1, \ell_2])$ is uniform distribution on interval $[\ell_1, \ell_2]$.

| | |
|--------------------|---|
| Admittances | $b = U([-1, 0])$ [p.u.], $g = b \times U([0, 0.5])$ [p.u.] |
| Voltages | $V = U([0.95, 1.05])$ [p.u.], $\delta = U([-0.5, 0.5])$ [rad] |
| Interface settings | $d = U([1.5, 3])$, $m = U([0.4, 2])$ [sec.] |

TABLE III: Parameters of the IEEE 33-bus system.

| i | 1 | 2 | 3 | 4 | 5 | 6 |
|-------------|--|-----|-----|-----|-----|-----|
| Bus index | 8 | 13 | 16 | 19 | 25 | 26 |
| DER type | DG | DG | DG | VSI | DG | VSI |
| d_i | 1.7 | 1.7 | 2 | 1 | 2 | 1.2 |
| m_i | 0.5 | 0.5 | 0.6 | 0.7 | 0.6 | 0.7 |
| Base values | $P_{\text{base}} = 100$ MW, $V_{\text{base}} = 12.66$ kV | | | | | |

III. The simulations are carried out in MATLAB.

Fig. 4 shows the spectrum of matrix J along with the value of $\mathcal{S}_i, \forall i \in \{1, \dots, 6\}$ under three different operating points referred to as Cases 1 to 3. In Case 1, $\mathcal{S}_i > 0$ for $i = 4$ and $i = 6$. Moreover, in Case 2, $\mathcal{S}_i > 0$ for $i = 6$. Case 3 is the only case where $\mathcal{S}_i \leq 0, \forall i \in \{1, \dots, 6\}$, and condition (12) guarantees that the system is asymptotically stable in this case. According to this figure, in all three cases the non-zero eigenvalues of J are located in the left half plane and the system is asymptotically stable. However, from Case 1 to Case 3, as we move towards satisfying $\mathcal{S}_i \leq 0, \forall i \in \{1, \dots, 6\}$, the magnitude of the imaginary parts of the eigenvalues in $\sigma(J)$ is reduced, and their real parts are mainly moved towards $-\infty$, thereby making the system less oscillatory. Indeed, a smaller value of \mathcal{S}_i (say when $\mathcal{S}_i > 0$) means the violation of constraint $\mathcal{S}_i \leq 0$ is smaller, and it is easier to enforce condition (12), and therefore to make sure we have reached stability. Evidently, the value of \mathcal{S}_i can be seen as a stability measure, i.e., it roughly indicates how stable the system is. This application of condition (12) was also shown in the four-microgrid test case in the previous section. Finally, Fig. 5 depicts the frequency trajectories of the system in Case 3, where condition (12) holds. As can be seen, after a transient, all frequency deviations converge to zero, and the EP, which was certified by Theorem 2, is asymptotically stable. The initial condition in this simulation is chosen arbitrary within a reasonable range.

C. Larger-Scale Systems

Next, we test the proposed stability certificate on a set of large-scale synthetic networks. Figs. 6b and 6e show two examples of such multi- μG networks consisting of 50 and 100 microgrids, respectively. The network graphs are randomly generated, the sparsity patterns of their adjacency matrix are depicted in Figs. 6a and 6d, and the corresponding static and dynamic parameters are given Table II. Note also that the diameter (i.e., the longest graph geodesic) of the graphs 6b and 6e are 6 and 8, respectively. Adopting the aforementioned distributed control rule, each microgrid adjusts its controller parameters d_i and m_i (within the permissible range) to meet condition (8). Obeying this rule at an EP guarantees that all nonzero eigenvalues of the Jacobian matrix J have negative real part, and consequently, the EP is locally asymptotically stable (see Figs. 6c and 6f).

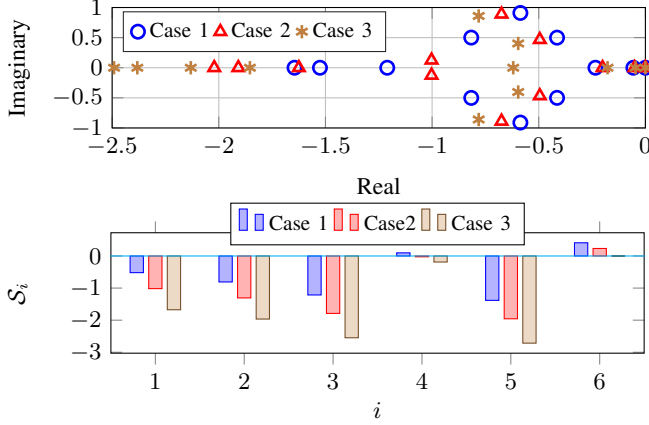


Fig. 4: Illustration of stability certificate on the IEEE 33-bus system. (a) Spectrum of matrix J . (b) Value of stability index S_i in different buses.

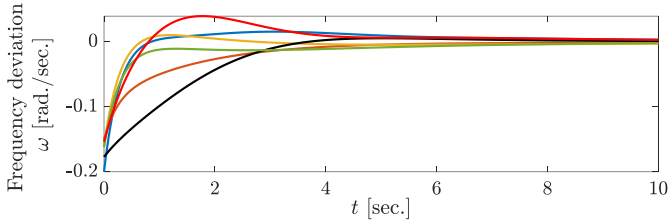


Fig. 5: Trajectories of the frequency deviation ω_i for 6 DERs in the IEEE 33-bus system.

VI. CONCLUSIONS

This paper proposes new stability certificates for the small-signal stability of multi- μ Gs. In particular, we prove in Theorem 1 that an EP of a multi- μ G system is locally asymptotically stable if either i) the network is lossless; or ii) in a lossy network, a local condition (i.e., condition (8)) is satisfied at each microgrid PCC/DER, which roughly speaking requires:

$$\left(\frac{\text{Reactive power}}{\text{absorption}} \right) + \frac{\text{Voltage magnitude}}{\text{Line reactance}} \leq \frac{\text{Damping}^2}{2 \cdot \text{Inertia}}.$$

This condition sheds new light on the interplay of system stability, network topology, and dynamic parameters. It also provides a fully distributed control scheme that is guaranteed to stabilize the multi- μ G system. The new certificate also reveals an analog of Braess's Paradox in multi- μ G control that adding more lines in the linking grid may worsen system stability, and switching off lines may improve stability margin. The proposed condition in Theorems 1 and 2 can improve the situational awareness of system operators by providing a fast stability certificate as well as showing how different corrective actions would make the EP stable. In the literature, several stability criteria are developed based on various dynamical models, focusing on different aspects of stability. Finding a proper way to compare and merge these criteria and deriving a unified stability criterion will be an interesting direction for future work, and the framework proposed in [28]–[30] is a promising step towards this direction.

APPENDIX A

PROOF OF PROPOSITION 1

proof of (i). Let $(v_1, v_2) \in \ker(J)$ where $v_1, v_2 \in \mathbb{R}^n$. Then

$$\begin{bmatrix} 0 & I \\ -M^{-1}L & -M^{-1}D \end{bmatrix} \begin{bmatrix} v_1 \\ v_2 \end{bmatrix} = 0, \quad (13)$$

which implies that $v_2 = 0$ and $M^{-1}Lv_1 = 0$. Since M is non-singular, $Lv_1 = 0$, i.e. $v_1 \in \ker(L)$. Therefore, $\text{proj}(\ker(J)) \subseteq \ker(L)$. Conversely, let $v_1 \in \ker(L)$. Set $v_2 = 0$. Then $(v_1, v_2) \in \ker(J)$ as it satisfies (13). \square

proof of (ii) and (iii). From part (i) of this proposition, we know that $(v, 0) \in \ker(J) \iff v \in \ker(L)$. Therefore, $\{(v_1, 0), \dots, (v_m, 0)\}$ is a set of linearly independent eigenvectors in $\ker(J)$ if and only if $\{v_1, \dots, v_m\}$ is a set of linearly independent eigenvectors in $\ker(L)$, i.e., $\dim(\ker(J)) = \dim(\ker(L))$. Finally, part (iii) is an immediate consequence of either of the first two parts. \square

APPENDIX B

PROOF OF THEOREM 1

proof of (a). This is an immediate consequence of Propositions 1 and 2. \square

proof of (b). See [36, Proof of Theorem 1]. \square

proof of (c). The result holds for real nonzero eigenvalues of J , as shown in the previous part. Now let $\lambda \in \mathbb{C}, \lambda \in \sigma(J)$, then according to Lemma 2, $\exists v \in \mathbb{C}^n, v \neq 0$ such that

$$(L + \lambda D + \lambda^2 M)v = 0. \quad (14)$$

It is always possible to normalize v such that $\max_{i \in \mathcal{N}} |v_i| = 1$. Here and in the rest of this proof, if $x \in \mathbb{C}$, then $|x|$ denotes the modulus of x . Let $k := \text{argmax}_{i \in \mathcal{N}} |v_i|$, and spell out the k -th row of (14):

$$L_{kk}v_k + \lambda d_k v_k + \lambda^2 m_k v_k = - \sum_{i=1, i \neq k}^n L_{ki} v_i. \quad (15)$$

Using the triangle inequality, we have

$$\left| - \sum_{i=1, i \neq k}^n L_{ki} v_i \right| \leq \sum_{i=1, i \neq k}^n |L_{ki}| |v_i| \leq \sum_{i=1, i \neq k}^n |L_{ki}|.$$

Define $\mathcal{R} := \sum_{i=1, i \neq k}^n |L_{ki}|$. Now assume that $\lambda = \alpha + j\beta$ with $\alpha \geq 0, \beta \neq 0$ is a nonzero eigenvalue of J , and let us lead this assumption to a contradiction. Recall $|v_k| = \|v\|_\infty = 1$. Equation (15) implies that

$$\begin{aligned} \mathcal{R}^2 &\geq |L_{kk}v_k + \lambda d_k v_k + \lambda^2 m_k v_k|^2 = |L_{kk} + \lambda d_k + \lambda^2 m_k|^2 \\ &= L_{kk}^2 + (\alpha d_k + (\alpha^2 - \beta^2)m_k)^2 + 2L_{kk}(\alpha d_k + \alpha^2 m_k) \\ &\quad - 2L_{kk}\beta^2 m_k + 4\alpha^2 \beta^2 m_k^2 + \beta^2 d_k^2 + 4\alpha \beta^2 m_k d_k. \end{aligned}$$

Recall that if $(\delta^*, \omega^*) \in \Omega$, matrix L has zero row sum, i.e., $\mathcal{R} = L_{kk}$. By cancelling \mathcal{R}^2 and L_{kk}^2 terms and moving $2L_{kk}\beta^2 m_k$ and $\beta^2 d_k^2$ to the left-hand side, we arrive at

$$\begin{aligned} \beta^2(2L_{kk}m_k - d_k^2) &\geq (\alpha d_k + (\alpha^2 - \beta^2)m_k)^2 \\ &\quad + 2L_{kk}(\alpha d_k + \alpha^2 m_k) \\ &\quad + 4\alpha^2 \beta^2 m_k^2 + 4\alpha \beta^2 m_k d_k. \end{aligned} \quad (16)$$

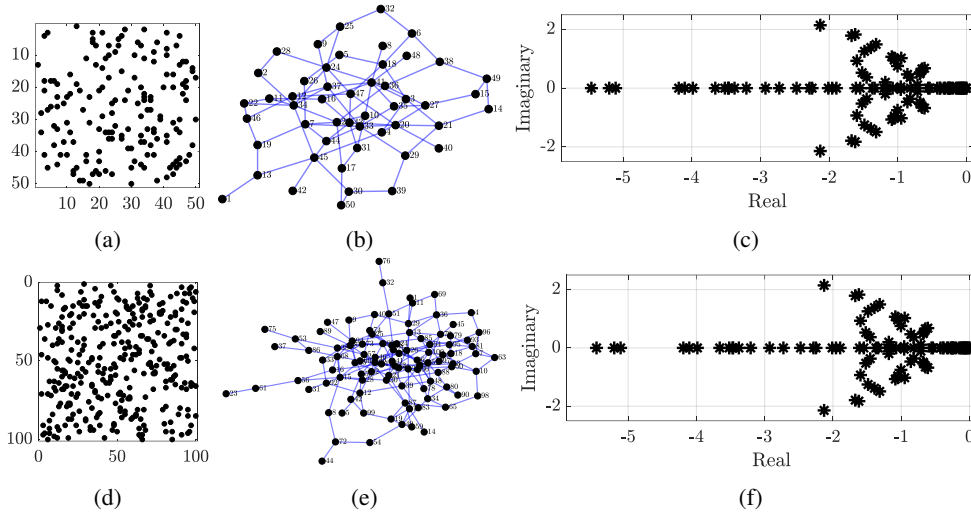


Fig. 6: Synthetic multi- μ G networks satisfying condition (8). (a) Sparsity pattern of the 50-microgrid adjacency matrix, black points are ones. (b) 50-microgrid network. (c) Eigenvalues of the 50-microgrid network. (d) Sparsity pattern of the 100-microgrid adjacency matrix, black points are ones. (e) 100-microgrid network. (f) Eigenvalues of the 100-microgrid network.

Now, note that the outgoing reactive power flow at PCC k is

$$\begin{aligned}
 Q_k &= -\sum_{i=1}^n V_k V_i Y_{ki} \sin(\theta_{ki} - \delta_k^* + \delta_i^*) \\
 &= -V_k^2 B_{kk} - \sum_{i=1, i \neq k}^n V_k V_i Y_{ki} \sin(\theta_{ki} - \delta_k^* + \delta_i^*) \\
 &= -V_k^2 B_{kk} - L_{kk}, \tag{17}
 \end{aligned}$$

where $B_{kk} = Y_{kk} \sin(\theta_{kk})$. Therefore condition (8) implies that $(2L_{kk}m_k - d_k^2) \leq 0$, thus the left-hand side of the inequality (16) is nonpositive. If $\alpha \geq 0$ and $\beta \neq 0$, the right-hand side of (16) will be positive, which is the desired contradiction. According to Proposition 1, the simple zero eigenvalue of the Jacobian matrix J stems from the translational invariance of the flow function (2). As mentioned earlier, we can eliminate this eigenvalue by choosing a reference bus and refer all other bus angles to it. Therefore, the set of EPs $\{\delta^* + \alpha \mathbf{1} : \alpha \in \mathbb{R}\}$ will collapse into one EP. Such an EP will be asymptotically stable. \square

proof of (d). Let $\lambda \in \sigma(J)$, then according to Lemma 2, $\exists v \neq 0$ such that $(L + \lambda D + \lambda^2 M)v = 0$. According to part (b) of this proof, if the eigenvalue λ is a real number, the desired result holds. We complete the proof in two steps:

Step 1: First, we prove that the eigenvalues of J cannot be purely imaginary. Suppose $\lambda = j\beta \in \sigma(J)$ for some nonzero real β . Let $v = x + jy$, then $((L - \beta^2 M) + j\beta D)(x + jy) = 0$, which can be equivalently written as

$$\begin{bmatrix} L - \beta^2 M & -\beta D \\ \beta D & L - \beta^2 M \end{bmatrix} \begin{bmatrix} x \\ y \end{bmatrix} = \begin{bmatrix} 0 \\ 0 \end{bmatrix}. \tag{18}$$

Define the matrix

$$H(\beta) := \begin{bmatrix} \beta D & L - \beta^2 M \\ L - \beta^2 M & -\beta D \end{bmatrix}. \tag{19}$$

For a lossless network, $L \succeq 0$ (see Section III-C). Thus, $H(\beta)$ is a symmetric matrix. Since $D \succ 0$, the determinant of $H(\beta)$ can be expressed using Schur complement as

$$\begin{aligned}
 \det(H(\beta)) &= \det(-\beta D) \det(\beta D) \\
 &\quad + \beta^{-1} (L - \beta^2 M) D^{-1} (L - \beta^2 M).
 \end{aligned}$$

Define the following matrices for the convenience of analysis:

$$\begin{aligned}
 A(\beta) &:= L - \beta^2 M, \\
 B(\beta) &:= D^{-1/2} A(\beta) D^{-1/2}, \\
 E(\beta) &:= I + \beta^{-2} B(\beta)^2.
 \end{aligned}$$

The inner matrix of the Schur complement can be written as

$$\begin{aligned}
 &\beta D + \beta^{-1} (L - \beta^2 M) D^{-1} (L - \beta^2 M) \\
 &= \beta D^{1/2} (I + \beta^{-2} D^{-1/2} A(\beta) D^{-1/2} A(\beta) D^{-1/2}) D^{1/2} \\
 &= \beta D^{1/2} (I + \beta^{-2} B(\beta)^2) D^{1/2} = \beta D^{1/2} E(\beta) D^{1/2}.
 \end{aligned}$$

Notice that $E(\beta)$ and $B(\beta)$ have the same eigenvectors and the eigenvalues of $E(\beta)$ and $B(\beta)$ have a one-to-one correspondence: μ is an eigenvalue of $B(\beta)$ if and only if $1 + \beta^{-2} \mu^2$ is an eigenvalue of $E(\beta)$. Indeed, we have $E(\beta)v = v + \beta^{-2} B(\beta)^2 v = v + \beta^{-2} \mu^2 v = (1 + \beta^{-2} \mu^2)v$ for any eigenvector v of $B(\beta)$ with eigenvalue μ . Since $B(\beta)$ is symmetric, μ is a real number. Hence, $E(\beta)$ is positive definite (because $1 + \beta^{-2} \mu^2 > 0$), therefore $H(\beta)$ is nonsingular for any real nonzero β . Then the eigenvector $v = x + jy$ is zero which is a contradiction. This proves that J has no eigenvalue on the punctured imaginary axis.

Step 2: Second, for a complex eigenvalue $\alpha + j\beta$ of J with $\alpha \neq 0, \beta \neq 0$, by setting $v = x + jy$, the pencil singularity equation becomes

$$(L + (\alpha + j\beta)D + (\alpha^2 - \beta^2 + 2\alpha\beta j)M)(x + jy) = 0.$$

Similar to Step 1 of the proof, define the matrix $H(\alpha, \beta)$ as

$$\begin{bmatrix} L + \alpha D + (\alpha^2 - \beta^2)M & -\beta(D + 2\alpha M) \\ \beta(D + 2\alpha M) & L + \alpha D + (\alpha^2 - \beta^2)M \end{bmatrix}.$$

We only need to consider two cases, namely i) $\alpha > 0, \beta > 0$ or ii) $\alpha < 0, \beta > 0$. For the first case, $\beta(D + 2\alpha M)$ is invertible and positive definite, therefore, we only need to look at the invertibility of the Schur complement

$$S(\alpha, \beta) + T(\alpha, \beta)S^{-1}(\alpha, \beta)T(\alpha, \beta),$$

where $S(\alpha, \beta) := \beta(D + 2\alpha M)$ and $T(\alpha, \beta) := L + \alpha D + (\alpha^2 - \beta^2)M$. Using the same manipulation as in Step 1 of the proof, we can see that the Schur complement is always invertible for any $\alpha > 0, \beta > 0$. This implies the eigenvector v is 0, which is a contradiction. Therefore, the first case is not possible. So any complex nonzero eigenvalue of J has negative real part. \square

APPENDIX C PROOF OF LEMMA 3

Proof. Consider the nodal admittance matrix $Y \in \mathbb{C}^{n \times n}$ which satisfies Assumptions 1 and 2. Let Y induce a network $\mathcal{G} = (\mathcal{N}, \mathcal{E})$ with the set of active nodes $\alpha \subset \mathcal{N}$ and passive nodes $\beta = \mathcal{N} \setminus \alpha$. According to Definition 2, the Kron reduced matrix after removing node $k_0 \in \beta$ is $Y^r \in \mathbb{C}^{(n-1) \times (n-1)}$ defined as

$$Y_{ik}^r = Y_{ik} - Y_{ik_0}Y_{k_0k}/Y_{k_0k_0}, \quad \forall i, k \neq k_0 \quad (20)$$

First, we prove that Y^r satisfies Assumption 1. Recall that the following two classes of matrices are invariant under Kron reduction [46]: i) matrices with zero row sum; ii) symmetric matrices. In other words, Y^r is a symmetric matrix with zero row sum. Hence, we can restrict our analysis to off-diagonal entries, and aim to prove that $Y^r = G^r + jB^r$ satisfies $G_{ik}^r \leq 0, B_{ik}^r \geq 0$, for all $i \neq k$. Consider $Y_{ik} = G_{ik} + jB_{ik}$ with $G_{ik} \leq 0$ and $B_{ik} \geq 0$ and note that for off-diagonal entries $Y_{ik}^r, i \neq k$, we have

$$\begin{aligned} Y_{ik} - Y_{ik}^r &= Y_{ik_0}Y_{k_0k}/Y_{k_0k_0} \\ &= (G_{ik_0} + jB_{ik_0})(G_{k_0k} + jB_{k_0k})/(G_{k_0k_0} + jB_{k_0k_0}) \\ &= ((G_{ik_0}G_{k_0k} - B_{ik_0}B_{k_0k}) \\ &\quad + j(G_{ik_0}B_{k_0k} + B_{ik_0}G_{k_0k}))(G_{k_0k_0} - jB_{k_0k_0})/\eta, \end{aligned}$$

where $\eta = G_{k_0k_0}^2 + B_{k_0k_0}^2$. Observe that

$$\begin{aligned} \Im(Y_{ik_0}Y_{k_0k}/Y_{k_0k_0})\eta &= G_{k_0k_0}G_{ik_0}B_{k_0k} + G_{k_0k_0}B_{ik_0}G_{k_0k} \\ &\quad - B_{k_0k_0}(G_{ik_0}G_{k_0k} - B_{ik_0}B_{k_0k}) \leq 0, \end{aligned}$$

where the inequality holds because under Assumptions 1 and 2, we have

$$\begin{aligned} G_{k_0k_0}G_{ik_0}B_{k_0k} &\leq 0, G_{k_0k_0}B_{ik_0}G_{k_0k} \leq 0, \\ G_{ik_0}G_{k_0k} - B_{ik_0}B_{k_0k} &\leq 0, -B_{k_0k_0} \geq 0. \end{aligned}$$

This proves that $B_{ik}^r \geq 0$, for all $i \neq k$. Also observe that

$$\begin{aligned} \Re(Y_{ik_0}Y_{k_0k}/Y_{k_0k_0})\eta &= G_{k_0k_0}G_{ik_0}G_{k_0k} - G_{k_0k_0}B_{ik_0}B_{k_0k} \\ &\quad + B_{k_0k_0}G_{ik_0}B_{k_0k} + B_{k_0k_0}B_{ik_0}G_{k_0k} \\ &\geq G_{k_0k_0}G_{ik_0}G_{k_0k} - \nu_{\max}^2 G_{k_0k_0}G_{ik_0}G_{k_0k} \\ &\quad + \nu_{\min}^2 G_{k_0k_0}G_{ik_0}G_{k_0k} + \nu_{\min}^2 G_{k_0k_0}G_{ik_0}G_{k_0k} \\ &= (1 + 2\nu_{\min}^2 - \nu_{\max}^2)G_{k_0k_0}G_{ik_0}G_{k_0k} \geq 0, \end{aligned}$$

where the inequality holds because under Assumptions 1 and 2, we have $1 + 2\nu_{\min}^2 - \nu_{\max}^2 \geq 0$ and $G_{k_0k_0}G_{ik_0}G_{k_0k} \geq 0$. This shows that $G_{ik}^r \leq 0$ for all $i \neq k$, and completes the first part of proof. Next, we prove that $B_{kk}^r \geq B_{kk}$ for all $k \neq k_0$. Observe that

$$\Im(Y_{kk}^r - Y_{kk})\eta = (G_{kk_0}^2 - B_{kk_0}^2)B_{k_0k_0} - 2G_{k_0k_0}G_{kk_0}B_{k_0k_0}.$$

According to Assumption 1, we have $G_{k_0k_0} \geq 0, B_{k_0k_0} \leq 0, G_{kk_0} \leq 0, B_{kk_0} \geq 0, \forall k \neq k_0$. Assumption 2 says $|G_{kk_0}| \leq |B_{kk_0}|$. Hence $(G_{kk_0}^2 - B_{kk_0}^2)B_{k_0k_0} \geq 0$ and $-2G_{k_0k_0}G_{kk_0}B_{k_0k_0} \geq 0$. This implies that $B_{kk}^r \geq B_{kk}$, and completes the proof. \square

APPENDIX D PROOF OF THEOREM 2

Proof. Let the nodal admittance matrix of \mathcal{G}^d be $Y \in \mathbb{C}^{n \times n}$ which satisfies Assumptions 1 and 2. Suppose \mathcal{G}^d has the set of active nodes $\alpha \subset \mathcal{N}^d$ and passive nodes $\beta = \mathcal{N}^d \setminus \alpha$. After properly labeling the nodes, we can have $\beta = \{n - |\beta| + 1, \dots, n\}$. In order to get the admittance matrix Y^r of the Kron reduced network \mathcal{G}^r , we need to remove the set of passive nodes β according to Definition 2, and this can be accomplished by constructing a sequence of matrices $\{Y^{(\ell)}\}_{\ell=1}^{|\beta|}$, where $Y^{(\ell)} \in \mathbb{C}^{(n-\ell) \times (n-\ell)}$ is defined as

$$Y_{ik}^{(\ell)} = Y_{ik}^{(\ell-1)} - Y_{im_\ell}^{(\ell-1)}Y_{m_\ell k}^{(\ell-1)}/Y_{m_\ell m_\ell}^{(\ell-1)}, \quad (21)$$

where $i, k \in \{1, \dots, n - \ell\}$, $Y^{(0)} = Y$, $Y^{(|\beta|)} = Y^r$, and $m_\ell = n - \ell + 1$. Observe that the matrix sequence $\{Y^{(\ell)}\}_{\ell=1}^{|\beta|}$ is well-defined. Now, according to Lemma 3, for each $\ell \in \{1, \dots, |\beta|\}$ matrix $Y^{(\ell)}$ satisfies Assumptions 1. Hence, Y^r satisfies both Assumptions 1 and 2.

Next, Let $V \in \mathbb{C}^n$ and $S \in \mathbb{C}^n$ be the vector of nodal voltages and power injections of network \mathcal{G}^d , respectively. It can be shown that if the vector of nodal voltages of the reduced network \mathcal{G}^r is $V[\alpha]$, then the vector of power injections in the reduced network is $S[\alpha]$. Hence, if the voltage magnitudes in the original and Kron-reduced networks are equal, then the reactive power Q_i at active nodes in the two networks are equal.

Moreover, Lemma 3 asserts that $B_{ii}^{(\ell)} \geq B_{ii}^{(\ell-1)}$, for all $i \in \{1, \dots, n - \ell\}$. Since this inequality holds for all $\ell \in \{1, \dots, |\beta|\}$, by induction, we conclude that $B_{ii}^r \geq B_{ii}, \forall i \in \{1, \dots, n - |\beta|\}$ where B_{ii}^r and B_{ii} are the i th diagonal entries of the Kron-reduced and original admittance matrices, respectively. Note that $-Q_i - B_{ii}^r V_i^2 \leq -Q_i - B_{ii} V_i^2$. Therefore, if $-Q_i - B_{ii} V_i^2 \leq d_i^2/2m_i$ holds for active nodes in the original network, then $-Q_i - B_{ii}^r V_i^2 \leq \frac{d_i^2}{2m_i}$ also holds and according to Theorem 1, the stability of the system is guaranteed. \square

REFERENCES

- [1] Y. Zhang and L. Xie, "A transient stability assessment framework in power electronic-interfaced distribution systems," *IEEE Trans. Power Syst.*, vol. 31, no. 6, pp. 5106–5114, 2016.
- [2] A. Gholami and X. A. Sun, "Towards resilient operation of multimicrogrids: An MISOCP-based frequency-constrained approach," *IEEE Trans. Control Netw. Syst.*, vol. 6, no. 3, pp. 925–936, Sep. 2019.
- [3] J. Schiffer, D. Goldin, J. Raisch, and T. Sezi, "Synchronization of droop-controlled microgrids with distributed rotational and electronic generation," in *52nd IEEE Conf. Decision Control*, 2013, pp. 2334–2339.
- [4] Q.-C. Zhong and G. Weiss, "Synchronverters: Inverters that mimic synchronous generators," *IEEE Trans. Industrial Electronics*, vol. 58, no. 4, pp. 1259–1267, 2010.
- [5] T. L. Vu, H. D. Nguyen, J. Slotine, and K. Turitsyn, "Reconfigurable microgrid architecture for blackout prevention," <https://www.dropbox.com/s/06jk9li7jsh0ibp/Manuscript.pdf?dl=0>, 2019.
- [6] J. Zaborszky, G. Huang, B. Zheng, and T.-C. Leung, "On the phase portrait of a class of large nonlinear dynamic systems such as the power system," *IEEE Trans. Autom. Control*, vol. 33, no. 1, pp. 4–15, 1988.
- [7] H.-D. Chiang, *Direct Methods for Stability Analysis of Electric Power Systems: Theoretical Foundation, BCU Methodologies, and Applications*. John Wiley & Sons, 2011.
- [8] P. Varaiya, F. F. Wu, and R.-L. Chen, "Direct methods for transient stability analysis of power systems: Recent results," *Proc. IEEE*, vol. 73, no. 12, pp. 1703–1715, 1985.
- [9] M. Anghel, F. Milano, and A. Papachristodoulou, "Algorithmic construction of lyapunov functions for power system stability analysis," *IEEE Trans. Circuits Syst. I: Reg. Papers*, vol. 60, no. 9, pp. 2533–2546, 2013.
- [10] S. Kundu and M. Anghel, "A multiple-comparison-systems method for distributed stability analysis of large-scale nonlinear systems," *Automatica*, vol. 78, pp. 25–33, 2017.
- [11] T. L. Vu and K. Turitsyn, "A framework for robust assessment of power grid stability and resiliency," *IEEE Trans. Autom. Control*, vol. 62, no. 3, pp. 1165–1177, 2016.
- [12] H.-D. Chiang, "Study of the existence of energy functions for power systems with losses," *IEEE Trans. Circuits Syst.*, vol. 36, no. 11, pp. 1423–1429, 1989.
- [13] N. Narasimhamurthi, "On the existence of energy function for power systems with transmission losses," *IEEE Trans. Circuits Syst.*, vol. 31, no. 2, pp. 199–203, 1984.
- [14] H. Kwatny, L. Bahar, and A. Pasrija, "Energy-like lyapunov functions for power system stability analysis," *IEEE Trans. Circuits Syst.*, vol. 32, no. 11, pp. 1140–1149, 1985.
- [15] H. R. Pota and P. J. Moylan, "A new lyapunov function for interconnected power systems," in *28th IEEE Conf. Decision Control*, 1989, pp. 2181–2185.
- [16] T. Athay, R. Podmore, and S. Virmani, "A practical method for the direct analysis of transient stability," *IEEE Trans. Power App. Syst.*, no. 2, pp. 573–584, 1979.
- [17] F. H. Silva, L. F. C. Alberto, J. B. London, and N. G. Bretas, "Smooth perturbation on a classical energy function for lossy power system stability analysis," *IEEE Trans. Circuits Syst. I: Reg. Papers*, vol. 52, no. 1, pp. 222–229, 2005.
- [18] C. Jozs, D. K. Molzahn, M. Tacchi, and S. Sojoudi, "Transient stability analysis of power systems via occupation measures," in *IEEE Conf. Innov. Smart Grid Technol.*, Washington, DC, USA, Feb. 2019.
- [19] R. Ortega, M. Galaz, A. Astolfi, Y. Sun, and T. Shen, "Transient stabilization of multimachine power systems with nontrivial transfer conductances," *IEEE Trans. Autom. Control*, vol. 50, no. 1, pp. 60–75, 2005.
- [20] S. J. Skar, "Stability of power systems and other systems of second order differential equations," Ph.D. dissertation, Dept. Math., Iowa State Univ., Iowa, USA, 1980.
- [21] J. A. Torres and S. Roy, "Graph-theoretic analysis of network input-output processes: Zero structure and its implications on remote feedback control," *Automatica*, vol. 61, pp. 73–79, 2015.
- [22] K. Koorehdavoudi, M. Hatami, S. Roy, V. Venkatasubramanian, P. Pantiaci, F. Xavier, and J. A. Torres, "Input-output characteristics of the power transmission network's swing dynamics," in *55th IEEE Conf. Decision Control*, 2016, pp. 1846–1852.
- [23] F. Ebrahimzadeh, M. Adeen, and F. Milano, "On the impact of topology on power system transient and frequency stability," in *EEEICI-ICPS Europe*. IEEE, 2019.
- [24] T. Ishizaki, A. Chakraborty, and J.-I. Imura, "Graph-theoretic analysis of power systems," *Proc. IEEE*, vol. 106, no. 5, pp. 931–952, 2018.
- [25] F. Dörfler, J. W. Simpson-Porco, and F. Bullo, "Electrical networks and algebraic graph theory: Models, properties, and applications," *Proc. IEEE*, vol. 106, no. 5, pp. 977–1005, 2018.
- [26] J. W. Simpson-Porco, F. Dörfler, and F. Bullo, "Synchronization and power sharing for droop-controlled inverters in islanded microgrids," *Automatica*, vol. 49, no. 9, pp. 2603–2611, 2013.
- [27] J. Schiffer, R. Ortega, A. Astolfi, J. Raisch, and T. Sezi, "Conditions for stability of droop-controlled inverter-based microgrids," *Automatica*, vol. 50, no. 10, pp. 2457–2469, 2014.
- [28] P. Vorobev, P.-H. Huang, M. Al Hosani, J. L. Kirtley, and K. Turitsyn, "A framework for development of universal rules for microgrids stability and control," in *56th IEEE Conf. Decision Control*. IEEE, 2017, pp. 5125–5130.
- [29] —, "Towards plug-and-play microgrids," in *44th Annu. Conf. IEEE Ind. Electron. Soc.*, 2018, pp. 4063–4068.
- [30] P.-H. Huang, P. Vorobev, M. Al Hosani, J. L. Kirtley, and K. Turitsyn, "Plug-and-play compliant control for inverter-based microgrids," *IEEE Trans. Power Syst.*, vol. 34, no. 4, pp. 2901–2913, 2019.
- [31] F. Paganini and E. Mallada, "Global analysis of synchronization performance for power systems: bridging the theory-practice gap," *IEEE Trans. Autom. Control*, vol. 65, no. 7, pp. 3007–3022, 2020.
- [32] C. Zhao, U. Topcu, N. Li, and S. Low, "Design and stability of load-side primary frequency control in power systems," *IEEE Trans. Autom. Control*, vol. 59, no. 5, pp. 1177–1189, 2014.
- [33] E. Weitenberg, Y. Jiang, C. Zhao, E. Mallada, C. De Persis, and F. Dörfler, "Robust decentralized secondary frequency control in power systems: Merits and tradeoffs," *IEEE Trans. Autom. Control*, vol. 64, no. 10, pp. 3967–3982, 2018.
- [34] A. S. Matveev, J. E. M. Martinez, R. Ortega, J. Schiffer, and A. Pyrkyn, "A tool for analysis of existence of equilibria and voltage stability in power systems with constant power loads," *IEEE Trans. Autom. Control*, 2020.
- [35] F. Dörfler and F. Bullo, "Synchronization and transient stability in power networks and nonuniform kuramoto oscillators," *SIAM J. Control Optimiz.*, vol. 50, no. 3, pp. 1616–1642, 2012.
- [36] A. Gholami and X. A. Sun, "A fast certificate for power system small-signal stability," in *59th IEEE Conf. Decision Control*, 2020, pp. 3383–3388, arXiv:2008.02263.
- [37] D. Braess, A. Nagurny, and T. Wakolbinger, "On a paradox of traffic planning," *Transportation Science*, vol. 39, no. 4, pp. 446–450, 2005.
- [38] V. Purba, B. B. Johnson, M. Rodriguez, S. Jafarpour, F. Bullo, and S. V. Dhople, "Reduced-order aggregate model for parallel-connected single-phase inverters," *IEEE Trans. Energy Convers.*, vol. 34, no. 2, pp. 824–837, 2019.
- [39] M. Khan, Y. Lin, B. Johnson, V. Purba, M. Sinha, and S. Dhople, "A reduced-order aggregated model for parallel inverter systems with virtual oscillator control," in *IEEE 19th Workshop Control Modeling for Power Electron. (COMPEL)*, 2018, pp. 1–6.
- [40] P. M. Anderson and A. A. Fouad, *Power System Control and Stability*. John Wiley & Sons, 2008.
- [41] X. Hou, Y. Sun, X. Zhang, J. Lu, P. Wang, and J. M. Guerrero, "Improvement of frequency regulation in vsg-based ac microgrid via adaptive virtual inertia," *IEEE Trans. Power Electron.*, vol. 35, no. 2, pp. 1589–1602, 2019.
- [42] R. D. Zimmerman and C. E. Murillo-Sanchez. MATPOWER. [Online]. Available: <https://matpower.org>
- [43] X. Wang, Y. Koç, R. E. Kooij, and P. Van Mieghem, "A network approach for power grid robustness against cascading failures," in *7th int. workshop on reliable networks design and modeling (RNDM)*, 2015, pp. 208–214.
- [44] A. Gholami, T. Shekari, and S. Grijalva, "Proactive management of microgrids for resiliency enhancement: An adaptive robust approach," *IEEE Trans. Sustain. Energy*, vol. 10, no. 1, pp. 470–480, 2017.
- [45] M. E. Baran and F. F. Wu, "Network reconfiguration in distribution systems for loss reduction and load balancing," *IEEE Trans. Power Del.*, vol. 4, no. 2, pp. 1401–1407, 1989.
- [46] F. Dörfler and F. Bullo, "Kron reduction of graphs with applications to electrical networks," *IEEE Trans. Circuits Syst. I: Reg. Papers*, vol. 60, no. 1, pp. 150–163, 2012.